

Role of Ce in enhanced performance of water oxidation reaction and urea oxidation reaction for NiFe Layered Double Hydroxide

Jianfeng Fan^a and Xiaoqiang Du^{b*}

^aDepartment of Chemistry, Xinzhou Normal University, Xinzhou 034000, People's Republic of China.

^bSchool of Chemical Engineering and Technology, North University of China, Xueyuan road 3, Taiyuan 030051, People's Republic of China. E-mail: duxq16@nuc.edu.cn

Turnover frequency (TOF) value of catalysts was calculated based on the equation: $\text{TOF} = (J \times A) / (4 \times F \times n)$, where J (mA/cm²) is the current density; A is the surface area of electrode (1 cm²); F is the Faraday constant (96485 C/mol); n is molar number of active sites on the electrode. Both Ni, Fe and Ce in NiFe LDH, Ce-NiFe LDH and Ce(OH)₃@NiFe LDH are regarded as active sites. The mass activity (MA) is calculated according to the equation: $\text{MA} = J/m$, where J (mA/cm²) is the current density at overpotential of 300 mV; m is the mass of active sites (Ni, Fe and Ce) deposited onto nickel foam.

Table S1. XPS fitting parameters for the binding energies of the resulting material.

Samples	Binding energy [eV]									
	Ni ²⁺		Ni ³⁺		Fe ³⁺		Ce ³⁺		Ce ⁴⁺	
	2p _{3/2}	2p _{1/2}	2p _{3/2}	2p _{1/2}	2p _{3/2}	2p _{1/2}	3d _{5/2}	3d _{3/2}	3d _{5/2}	3d _{3/2}
Ce(OH) ₃ @NiFe LDH	856.45	873.0	/	/	713.3	724.1	873.6	899.1	875.5	902.5
							879.1	905.0	881.3	907.8
									884.1	917.2
Ce-NiFe LDH	856.4	872.9	/	/	713.6	724.3	873.7	899.2	875.6	902.6
							879.2	905.1	881.4	907.9
									884.2	917.3
NiFe-LDH	856.3	872.8	/	/	714.0	724.5	/	/	/	/

Table S2. XPS fitting parameters for the Ce peak area of the resulting material.

Samples (Ce ³⁺ /Ce ⁴⁺ ratio)	Peak area			
	Ce ³⁺		Ce ⁴⁺	
	3d _{5/2}	3d _{3/2}	3d _{5/2}	3d _{3/2}
Ce(OH) ₃ @NiFe LDH	5648	4958	14539	5654
	6622	3790	3843	3248
			2479	4256
Ce-NiFe LDH	8137	2179	13954	15886
	21892	10237	5321	5347
			2742	2395

Table S3. Comparison of OER performances for Ce(OH)₃@NiFe LDH/NF with other reported electrocatalysts.

Electrocatalysts	Overpotential	References
Ce(OH)₃@NiFe LDH	220 mV at 10mA cm⁻²	This work
ZnCo LDH	325 mV at 10mA cm ⁻²	J. Mater. Chem. A, 2020,8, 8692-8699
NiCo ₂ S ₄ @NiFe LDH	201 mV at 60 mA cm ⁻²	ACS Appl. Mater. Interfaces 2017, 9, 15364–15372
CoO _x /FeO _x /CNT	308 mV at 10 mA cm ⁻²	J. Mater. Chem. A, 2020, 8, 15140–15147
NiS ₂ /NiSe ₂ nanocage	290 mV at 20 mA cm ⁻²	Small 2020, 16, 1905083
Co-Fe-V metal oxides	249 mV at 10 mA cm ⁻²	J. Mater. Chem. A, 2020, 8, 15951–15961
P-doped NiCo ₂ O ₄	300 mV at 10 mA cm ⁻²	ACS Appl. Mater. Interfaces 2020, 12, 2763–2772
NiS/Fe ₃ O ₄ HNPs@CNT	243 mV at 10 mA cm ⁻²	ACS Appl. Mater. Interfaces 2020, 12, 31552–31563
Fe ₃ O ₄ /FeS ₂	253 mV at 10 mA cm ⁻²	J. Mater. Chem. A, 2020, 8, 14145–14151
CoMoOS nanoboxes	281 mV at 10 mA cm ⁻²	Appl. Catal. B: Environ. 2020, 265, 118605
Ni ₅₉ Cu ₁₉ P ₉	307 mV at 10 mA cm ⁻²	Appl. Catal. B: Environ. 2018, 237, 409–415
Fe-Ni-P-B-O	236 mV at 10 mA cm ⁻²	ACS Nano 2019, 13, 12969–12979
hollow Fe-Co _x P	300 mV at 10 mA cm ⁻²	Chem. Eng. J. 2021, 409, 128227

Table S4. Comparison of UOR performances for Ce(OH)₃@NiFe LDH/NF with other reported electrocatalysts.

Catalyst	Electrolyte	potential	Ref
Ce(OH) ₃ @NiFe LDH	1 M KOH+0.5 M urea	1.40@10	This work
Fe ₂ P@Ni _x P/NF	1 M KOH+0.5 M urea	1.34@100	Chem. Eng. J., 2021,417, 128067
Fe _{11.1%} -Ni ₃ S ₂ /NF	1 M KOH+0.33 M urea	1.36@100	J. Mater. Chem. A, 2018, 6, 4346-4353
Mo-Ni ₃ S ₂	1 M KOH+0.3 M urea	1.37@100	J. Mater. Chem. A, 2021, 9, 3418-3426
V-Ni ₃ N	1 M KOH+0.5 M urea	1.39@100	J. Mater. Chem. A, 2021, 9, 4159-4166
Ni/FeOOH	1 M KOH+0.5 M urea	1.4@100	Chem. Commun., 2020, 56 ,14713-14716
Ni-S-Se/NF	1 M KOH+0.5 M urea	1.41@100	Nano Energy, 2021,81, 105605
CoS _x /Co-MOF	1 M KOH+0.5 M urea	1.42@100	Inorg. Chem. Front., 2020,7, 2602-2610
MNPBA-P	1 M KOH+0.5 M urea	1.43@100	ACS Sus. Chem. Eng., 2020,8, 16037-16045
Co-Z/Se-2	1 M KOH+0.5 M urea	1.44@100	J. Power Sources 2021,491, 229592

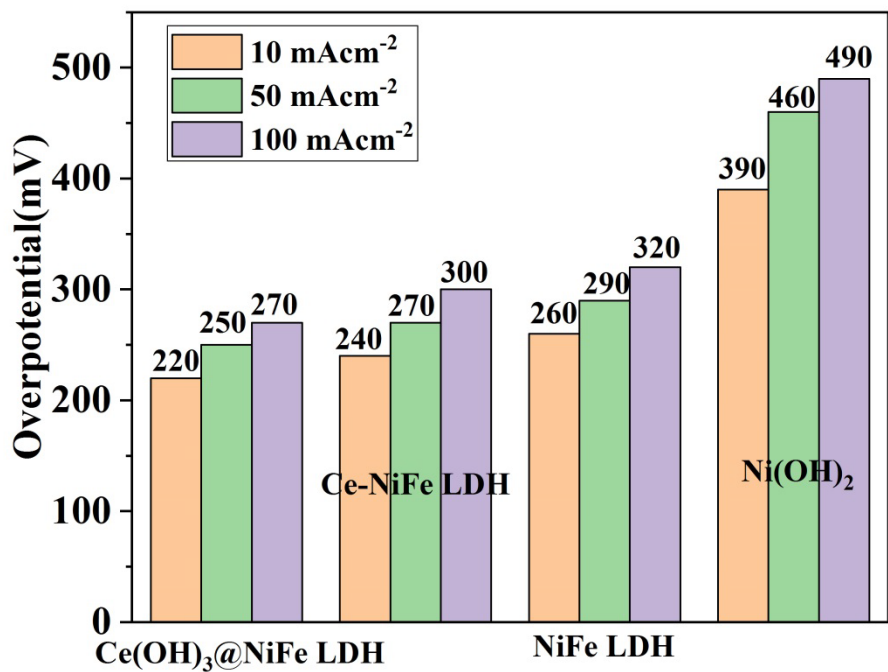


Fig. S1 The overpotential of Ni(OH)₂/NF, NiFe LDH/NF, Ce-NiFe LDH/NF and Ce(OH)₃@NiFe LDH/NF at 100 mA cm⁻² for OER.

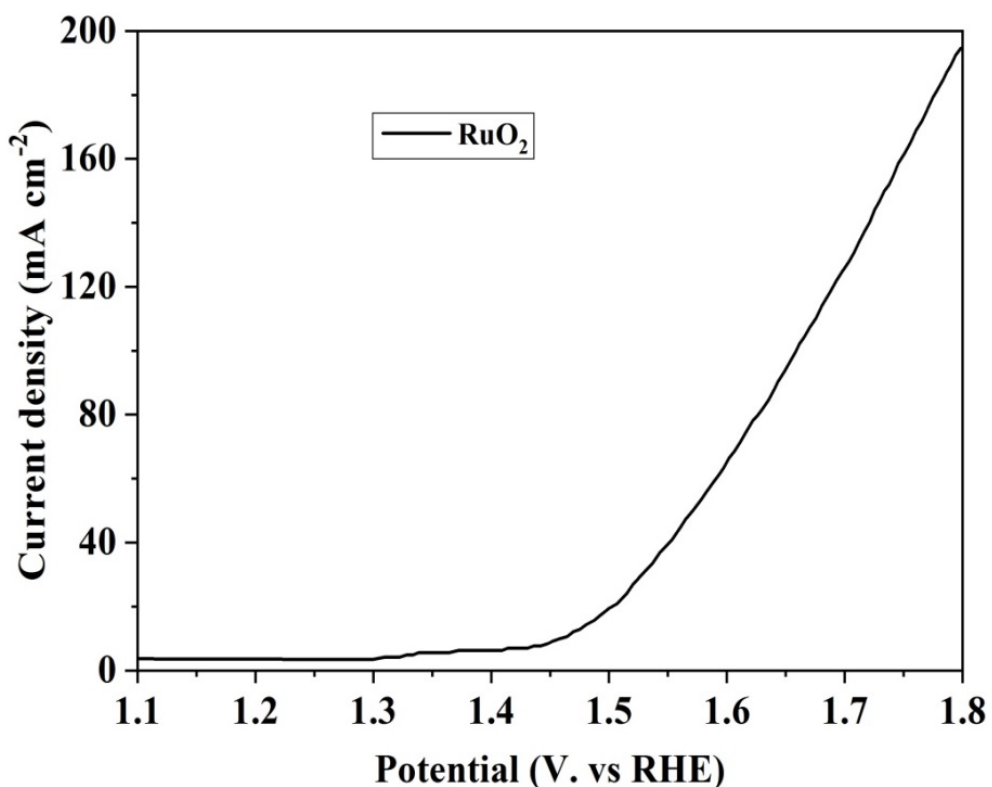


Fig. S2 Polarization curve of the RuO₂ for OER with a scan rate of 5 mV s⁻¹ in 1 M KOH.

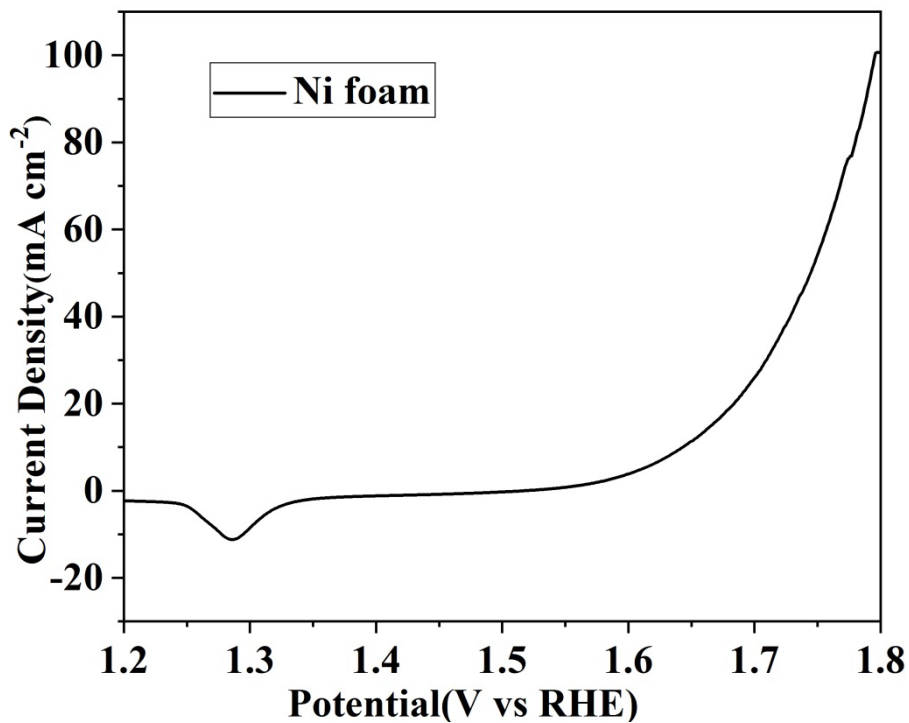


Fig. S3 Polarization curve of the Ni foam for OER with a scan rate of 5 mV s^{-1} in 1 M KOH.

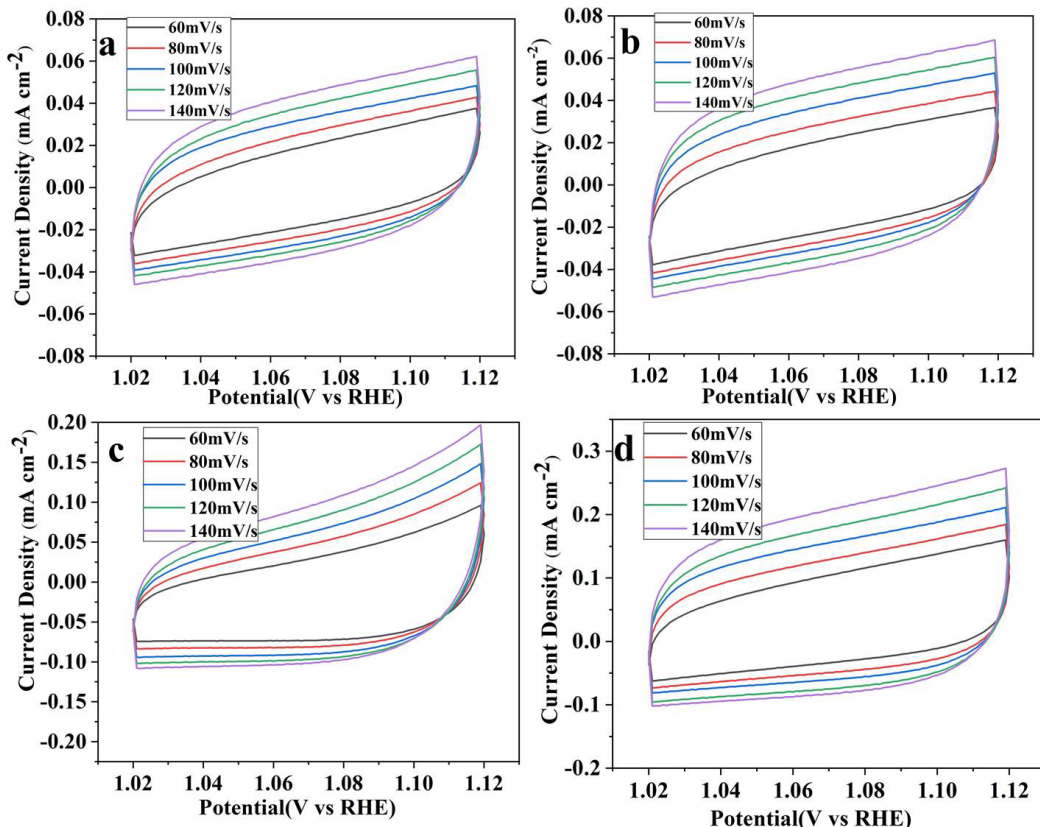


Fig. S4 CV curves with different scan rates for OER, Ni(OH)₂/NF (a), NiFe LDH/NF (b), Ce-NiFe LDH/NF (c) and Ce(OH)₃@NiFe LDH/NF (d).

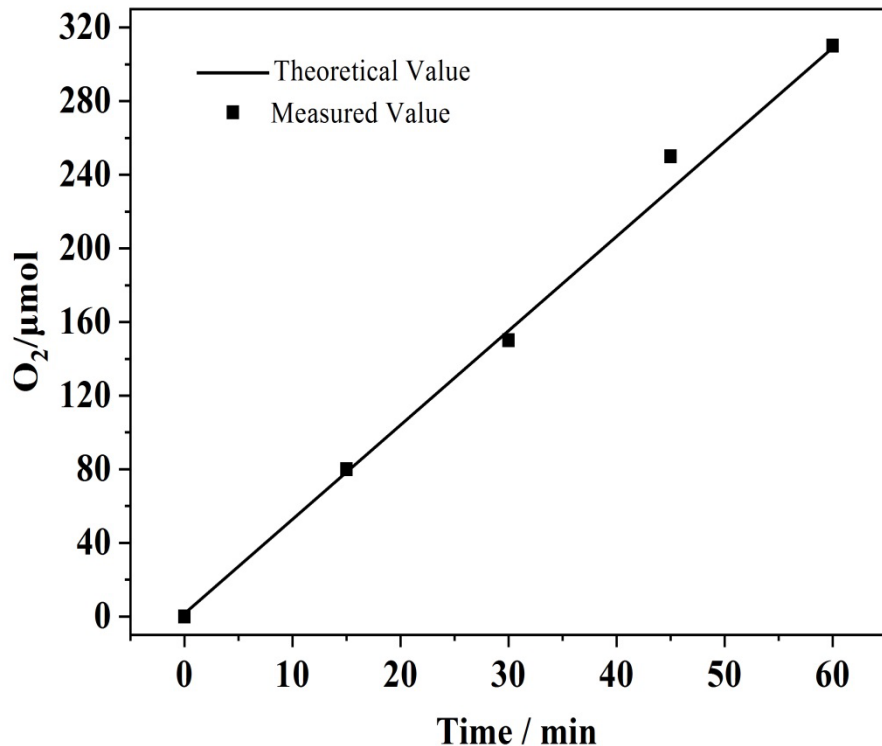


Fig. S5 Electrocatalytic efficiency of O_2 production over $\text{Ce}(\text{OH})_3@\text{NiFe LDH/NF}$.

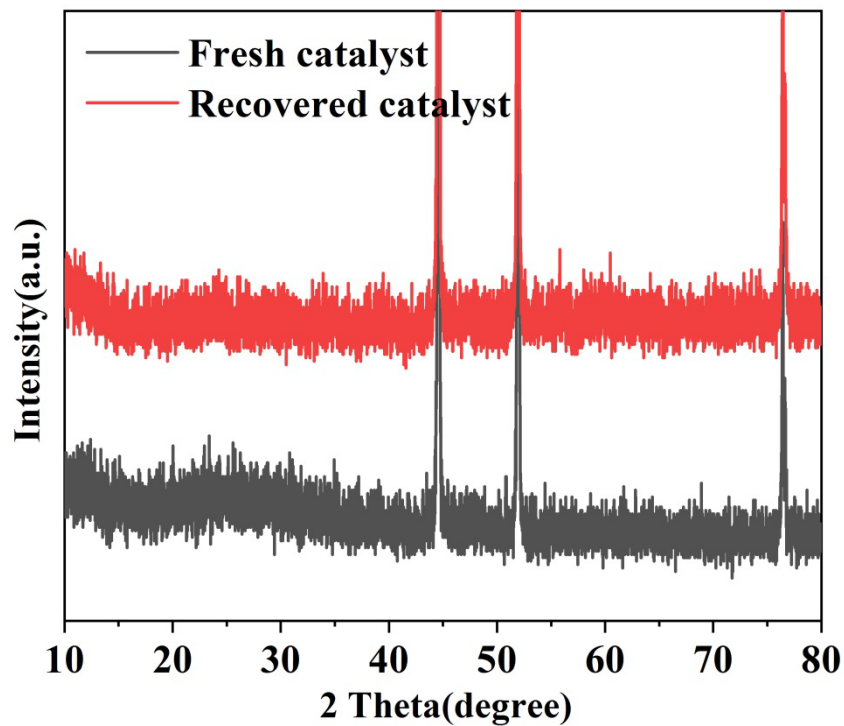


Fig. S6 XRD of fresh (a) and recovered (b) $\text{Ce}(\text{OH})_3@\text{NiFe LDH/NF}$ for OER.

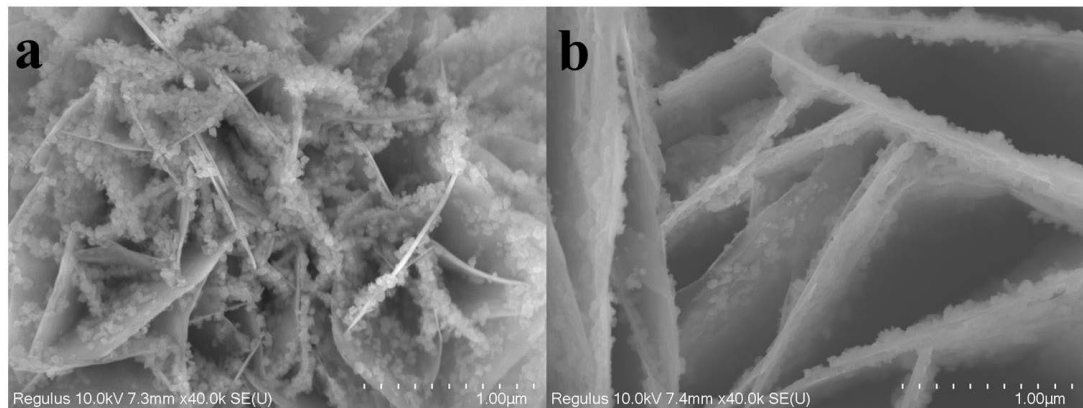


Fig. S7 SEM of fresh (a) and recovered (b) $\text{Ce}(\text{OH})_3@\text{NiFe LDH/NF}$ for OER.

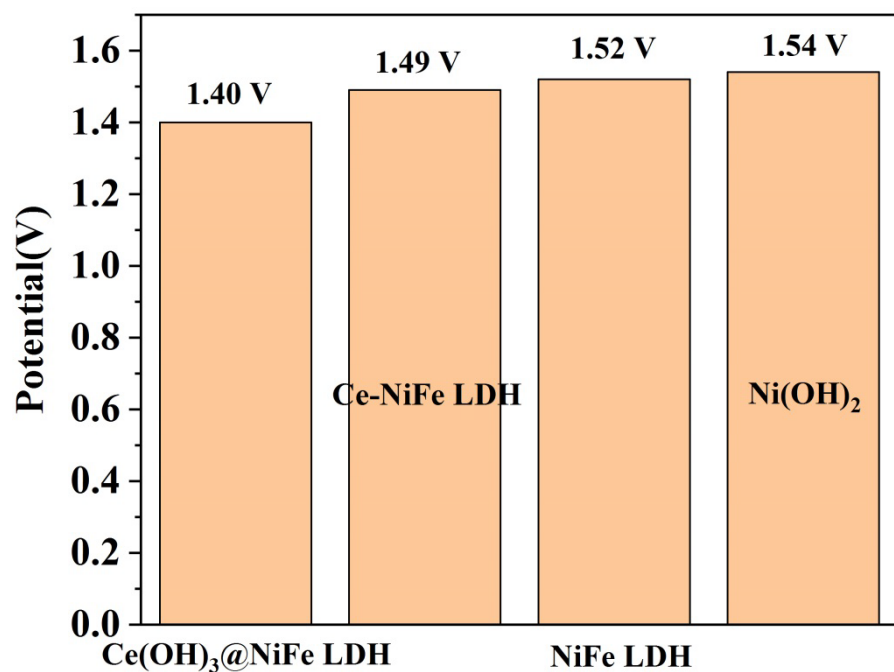


Fig. S8 The potential of $\text{Ni}(\text{OH})_2/\text{NF}$, NiFe LDH/NF , Ce-NiFe LDH/NF and $\text{Ce}(\text{OH})_3@\text{NiFe LDH/NF}$ at 10 mA cm^{-2} for UOR.

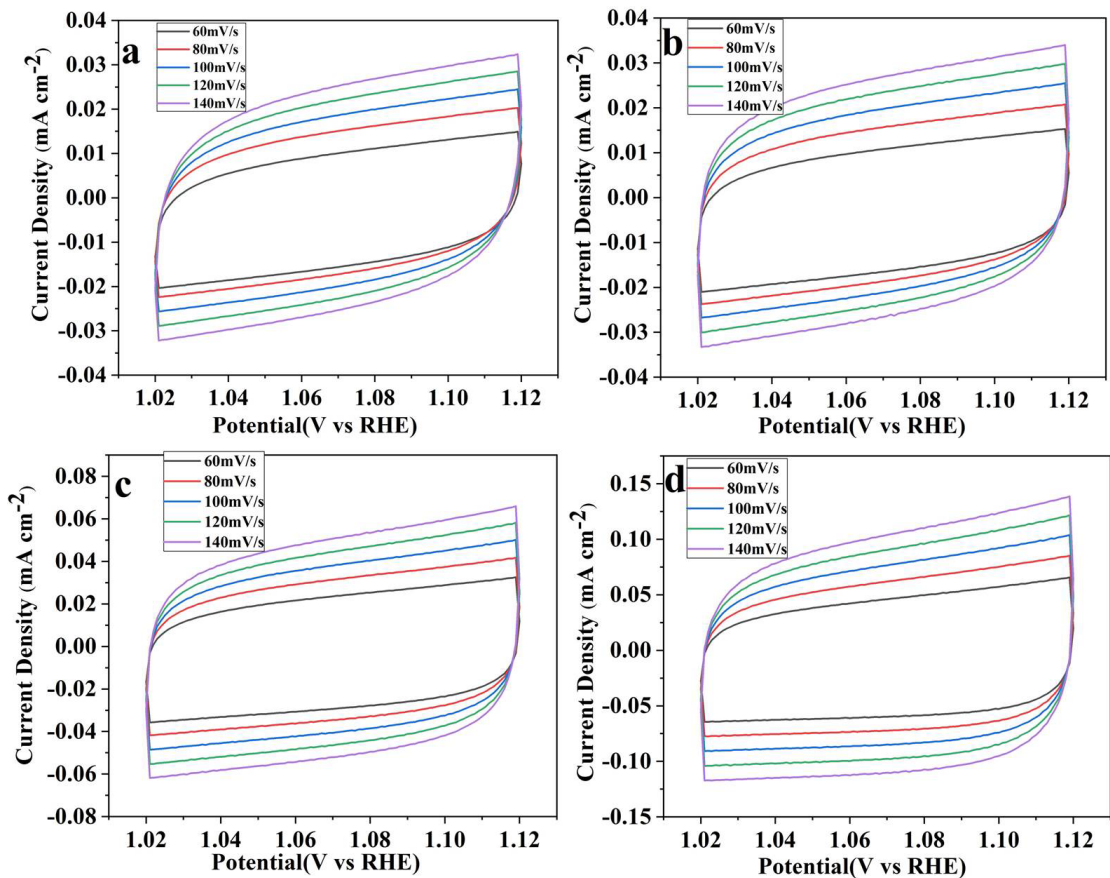


Fig. S9 CV curves with different scan rates for OER, Ni(OH)₂/NF (a), NiFe LDH/NF (b), Ce-NiFe LDH/NF (c) and Ce(OH)₃@NiFe LDH/NF (d).

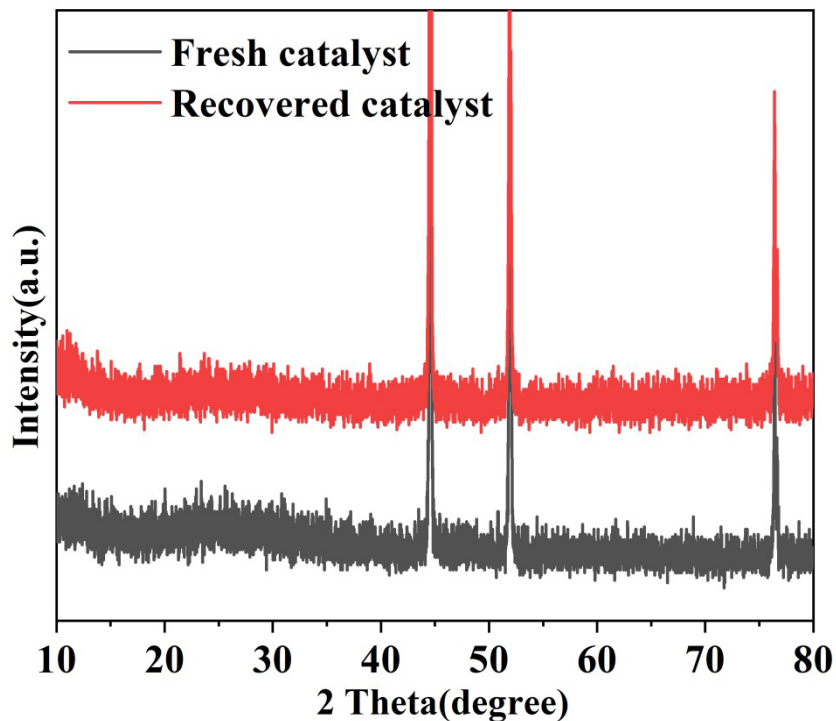


Fig. S10 XRD of fresh (a) and recovered (b) Ce(OH)₃@NiFe LDH/NF for UOR.

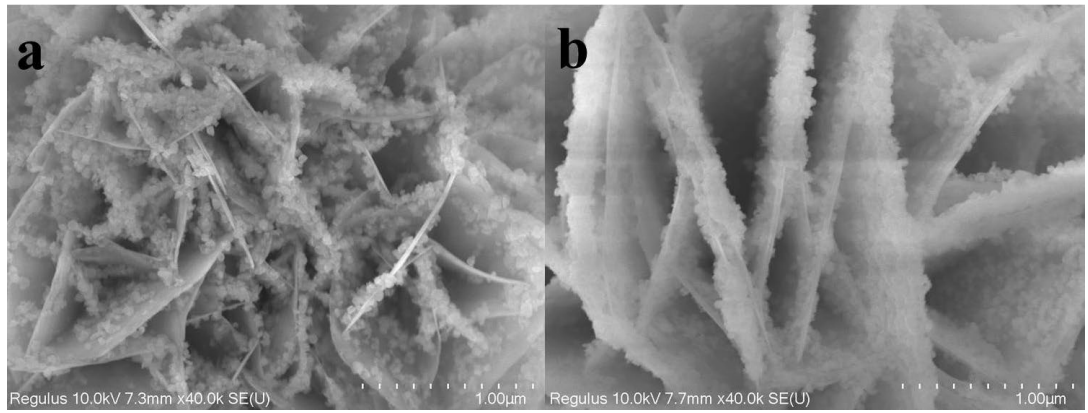


Fig. S11 SEM of fresh (a) and recovered (b) $\text{Ce}(\text{OH})_3@\text{NiFe}$ LDH/NF for UOR.